Bulletin of Earthquake Engineering
https://doi.org/10.1007/s10518-026-02373-4

ORIGINAL ARTICLE

Multi-performance parametric framework to enhance the design process and implementation of low-damage timber buildings

Giada Formichetti[1] · **Giuseppe Loporcaro**[2] · **Stefano Pampanin**[1]

Received: 14 July 2025 / Accepted: 16 January 2026

Abstract
The impact of catastrophic events like earthquakes and the challenges posed by climate change on the built environment have become a growing concern worldwide. Buildings should deal with multi-performance requirements through advanced and sustainable technological solutions able to withstand strong earthquakes with negligible damage. Moreover, the needs of modern society involve the design of "adaptive" or "flexible" buildings, allowing for several changes of use during their extended life-cycle with minimum disruptions, following a resilient approach. In this context, the low-damage post-tensioned laminated timber (Pres-Lam) technology represents a suitable solution towards a damage-control approach using modular components made of eco-friendly materials. Yet, even for this innovative solution, an optimized multi-performance-based design phase would be critical to enhance the building's resilience. This paper proposes a holistic integrated approach for the multi-performance design and evaluation of Pres-Lam buildings. A parametric framework is developed within the Rhino-Grasshopper platform to consider simultaneously seismic performance, energy efficiency and environmental footprint. The Multi-Objective Optimization technique is used to manage the conflicting goals towards the optimal solution, delivering adaptable, open-plan layouts in buildings with high seismic performance and low embodied and operational carbon emissions. The framework is applied to four different seismic and climatic scenarios, locating the building in Italy and New Zealand. Two Pareto-optimal solutions are selected and compared for each location, and their effective seismic performance is finally assessed by refined numerical analyses using a fragility-based approach. The research outcomes show the influence of different seismic hazards and climate on the whole-building performance, at the same time demonstrating the advantages of the Pres-Lam technology in delivering sustainable and resilient buildings.

Keywords Post-tensioned timber · Pres-Lam · Seismic safety · Sustainability · Energy efficiency · Integrated design

Extended author information available on the last page of the article

Published online: 24 February 2026

1 Introduction

The building sector is pivotal in fighting climate change, due to its cultural, economic, and environmental impact. Achieving a sustainable and resilient built environment is crucial for society's ability to realise the Sustainable Development Goals specified in the United Nations Agenda 2030 (United Nations 2015). However, to date, the construction sector is the largest contributor to Greenhouse Gases (GHGs) emissions and energy consumption, accounting for 37% of global energy-related Carbon Dioxide (CO_2) emissions and 36% of the total operational energy consumption (IEA 2021). At the recent 28th Conference of Parties (COP28), many countries proposed actions to decarbonise the building sector. The goal is to make clean technologies and sustainable solutions the most attractive option towards near-zero emissions buildings by 2030, as well as fostering an increased use of natural materials such as timber. Nevertheless, the recently-recognised high environmental impact of post-earthquake damage (Menna et al. 2013; FEMA 2018) and the vulnerability of modern "code-conforming" buildings highlighted by recent earthquakes (e.g., L'Aquila 2009, Canterbury sequence 2010–2011, Emilia 2012, Centre Italy 2016, Turkey & Syria 2023), show that seismic safety and environmental sustainability cannot be considered separately.

Targeting only Life-Safety criteria may not be enough, as it would result in severely damaged buildings which can be deemed as not cost-effective to be repaired, therefore leading to controlled demolition and reconstruction (Pampanin 2012, 2015). This represents an additional and significant source of carbon emissions (Belleri and Marini 2016). To overcome this issue related to the apparently inevitable equivalence between damage and ductility, the earthquake engineering community has been focusing on the development of innovative high performance technologies in the past twenty-five years, targeting a more appropriate damage-control design objective (Pampanin 2007). Among others, the low-damage PRESSS (PREcast Seismic Structural System) technology has been proposed and widely numerically and experimentally investigated in the past two decades, starting from the US-PRESSS programme in the 1990s at the University of California San Diego (UCSD), with further and significant developments and on site implementations at the University of Canterbury in New Zealand (Priestley 1991; Stanton et al. 1997; Priestley et al. 1999; NZCS 2010; Pampanin 2005, 2012). This technology replaces the traditional plastic hinge of monolithic solutions with a peculiar rocking-dissipative mechanism at the interface between the dry-jointed structural members. Unbonded post-tensioned cables/bars and internal mild steel or external fuse-type replaceable "Plug&Play" dissipaters (Sarti et al. 2016a) ensure respectively the re-centering and proper energy dissipation of the system, with negligible residual displacements (Pampanin et al. 2002). In the mid- 2000s, the same concept has been extended to laminated timber through the development of the Pres-Lam (Prestressed Laminated Timber) system (Palermo et al. 2005, 2006) (Fig. 1), combining the material's sustainability with the abovementioned high seismic performance. This technology integrates the fundamental concepts of circularity in construction, matching the necessary requirements in terms of standardization, demountability, reparability, reusability, and recyclability. At the same time, building components might be kept in use as long as possible thanks to the system's ability to withstand major earthquakes without any significant damage during its nominal (or extended) life. Additionally, different levels of design/use flexibility can be achieved, from the reversibility of internal spaces to the modifiability of structural and non-structural building components (Smith et al. 2011). It is therefore clear how this low-carbon and low-

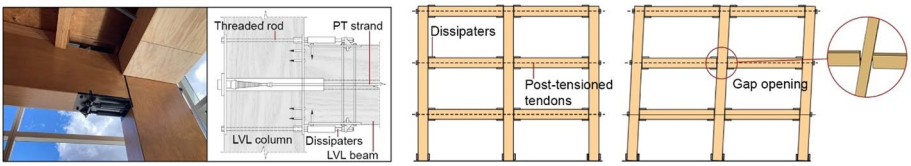

Fig. 1 Pres-Lam frame: detail of a beam-to-column connection (Merritt building, Christchurch, New Zealand, picture taken by the author), and the peculiar rocking mechanism

damage technology represents a competitive choice in a life-cycle thinking and resilient approach. Despite its relatively recent introduction in the construction sector worldwide, the Pres-Lam structural system has demonstrated its efficacy through extensive testing over the past two decades (Newcombe et al. 2010; Iqbal et al. 2010; Sarti et al. 2016b; Moroder et al. 2018; Pampanin et al. 2020), as well as in real buildings subjected to actual earthquakes (Smith et al. 2012; Holden et al. 2016; Granello et al. 2020).

To enhance community resilience and sustainability, choosing the right material and technology might not be enough. The design process should move towards an integrated approach, recognising the mutual influence between different buildings performance. To date, multi-disciplinary strategies for seismic and energy rehabilitation of existing buildings have been widely proposed. However, such approaches are not yet common practice for new design, especially in seismic-prone areas where the structural performance might jeopardize energy efficiency and environmental sustainability considerations in the decision-making process. On the other hand, many assessment tools are now available and well-established in the construction industry to evaluate the life-cycle environmental impacts of buildings. Within this context, the Life-Cycle Assessment (LCA) regulated by ISO 14,040 and ISO 14,044 (ISO 2006a, b) is to date the most comprehensive and, consequently, the most common procedure in the engineering practice. It represents a useful tool, especially in the early design stage, to evaluate different design options for new buildings. However, it is commonly used independently, while a multi-performance approach should rather be considered to handle different interrelated performance objectives and their trade-off. To this end, the Multi-Objective Optimization (MOO) has demonstrated a great potential to assist decision-makers towards higher performing early stage designs. Specifically, mathematical design optimization represents a valid alternative to the more traditional and time-consuming iterative-intuitive design approach. The latter is based mostly on the experience in achieving the "best possible" design option, with reference to predetermined targets/criteria/priorities, while the mathematical optimization allows to give a precise mathematical form to this concept. Of the different optimization methodologies available, evolutionary-based MOO using Genetic Algorithms (GA) has proven to be the most effective approach when tackling complex problems with a wide range of acceptable solutions (Holland 1975; Konak et al. 2006; Mueller and Ochsendorf 2015; Brown and Mueller 2016). The implementation of MOO could result in an increased interdisciplinary collaboration within the design process (Shen et al. 2018), also facilitating the identification of those objectives which contribute to the definition of a sustainable building. Despite its advantages, however, this methodology needs to be included within an accessible and automated process, in order to overcome its challenges in practical applications and facilitate the translation of mathematical models into real engineering problems.

Based on these considerations, this paper proposes a multi-performance parametric framework for the design and optimization of low-damage timber (Pres-Lam) buildings, by simultaneously considering seismic performance, environmental footprint, energy efficiency, and architectural flexibility. The framework is developed within the Rhino + Grasshopper platform (McNeel 2010), exploiting its parametric nature to seamlessly compute the objectives of the Multi-Objective Optimization (MOO). This enables the rapid exploration of a wide set of design solutions and the assessment of the trade-off between design objectives (i.e., building performance), while assuring the necessary compliance with the imposed constraints.

2 Methodology

A Grasshopper-based integrated parametric framework is proposed as shown in Fig. 2. Starting from the user-defined building parameters (e.g., geometry, structural and non-structural materials properties, seismic hazard, and climatic zone), the workflow allows for the model generation and the calculation of building performance. Specifically, a series of parallel automated algorithms are developed through independent software packages available in Grasshopper and Python-based modules for each of the building aspects considered: seismic design and analyses, environmental life-cycle assessment, energy modelling and simulations. These aspects become the objectives of the MOO package, which iteratively assesses a wide range of building configurations varying the input parameters in order to find the optimal solutions through an evolutionary approach.

The main workflow activities are listed and described below:

- *Structural seismic design*. The post-tensioned lateral force-resisting frames are designed through the Displacement-Based Design (DDBD) methodology proposed by Priestley (Priestley 2002; Priestley et al. 2007). The procedure is developed using the Python programming language within Grasshopper. Starting from the target/design displacement/drift as an input, the secant-to-target displacement of the equivalent single-degree-

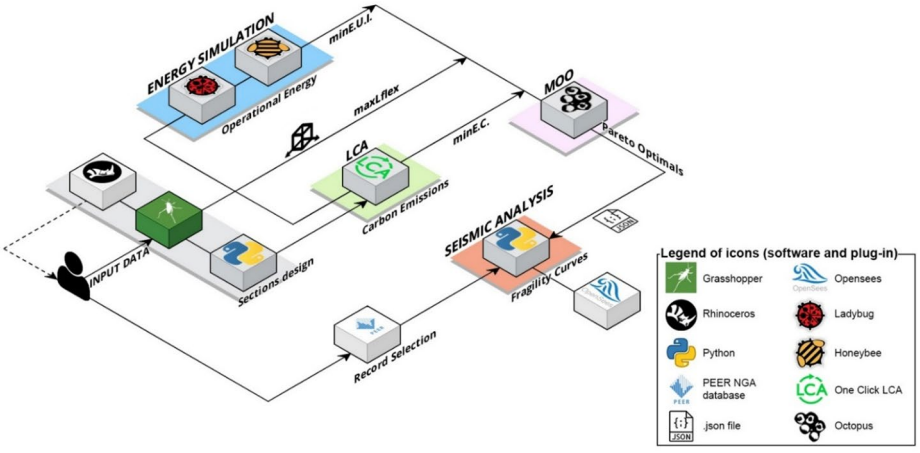

Fig. 2 Workflow of the multi-performance parametric framework for Pres-Lam buildings

of-freedom (SDOF) is derived. The effective period and the required Base Shear are subsequently calculated. The latter is distributed along the frame using the equilibrium approach proposed by Priestley et al. 2007 to obtain the internal actions. The structural members are then dimensioned at the Serviceability Limit State (SLS), which is usually the governing limit state for Pres-Lam structures. The number and dimensions of the external dissipaters and internal post-tensioned cables are consequently designed in detail and verified at the Ultimate Limit State (ULS) (Pampanin et al. 2013).

- *Life-Cycle Assessment (LCA)*. Using the extensive database of One Click LCA (Apellaniz et al. 2021), a Life-Cycle Assessment is performed considering the whole building (structural and non-structural components). As far as the calculation of the MOO objectives is concerned, the analysis is carried out from cradle-to-gate, i.e., from the extraction of raw materials to the factory supply (British Standard Institute 2011). However, a cradle-to-grave whole-life-cycle assessment is performed afterwards, also considering the construction phase, the operational energy used and the end-of-life scenario. Regarding the cradle-to-gate assessment, the Environmental Product Declarations (EPDs) of the project components are collected using either manufacturer-specific data or country-specific average data from One Click LCA database. The resulting Embodied Carbon (equivalent tons of Carbon Dioxide - tonCO2eq) is computed from the embodied carbon factors of each material relative to the mass or volume of the building elements directly mapped in Grasshopper. The cradle-to-grave assessment is finally executed using the One Click LCA cloud software, including the energy consumption obtained from the dynamic energy simulations and the end-of-life scenario for each building element. Specifically, recycling for steel and glass components is preferred, as well as the reuse of timber elements thanks to the use of a low-damage structural system.
- *Dynamic Energy Simulations*. Using the Ladybug's Honeybee Grasshopper plug-in (Roudsari and Pak 2013), the building energy model is generated by assigning material thermal properties (i.e., conductivity, density, and heat capacity), and boundary conditions to all the building components. Thermal zones are parametrically defined within the building, with different occupancy loads, equipment, lighting, and internal mass. Windows opening and closing are set by temperature setpoints for natural ventilation, while HVAC is assigned using a simplified Ideal Load System disregarding any inefficiency of the system. To accurately consider the actual impacts of heating and cooling systems, and therefore assess real energy consumption, it is essential to model a detailed HVAC system, incorporating a coefficient of performance. Nevertheless, using an ideal HVAC is still a reliable approach to estimate the building's operational energy consumption at an early stage (Bianchi et al. 2022). The external thermal load is determined by the climatic zone of the building's location, which is derived from data within EnergyPlus Weather (EPW) files imported via Ladybug. Dynamic energy simulations are then conducted using either Honeybee's EnergyPlus or OpenStudio software. Different outputs can be obtained from the analysis. In this study, the total (normalized) thermal annual load is considered, being the energy needed from cooling, heating, lights, and electric equipment to maintain a comfortable environment within the building (kWh/sqm/year). This output represents the operational energy input for the LCA from-cradle-to-grave analysis.
- *Multi-Objective Optimization*. The SPEA-2 (Strength-Pareto Evolutionary) Algorithm proposed by Zitzler et al. 2001 and contained in the Octopus plug-in for Grasshopper

is used for the Multi-Objective Optimization. This algorithm uses a regular population, and an external archive of a fixed size populated iteratively by non-dominated solutions as a form of elitism. For each solution within the pool, the objective values are calculated together with the SPEA-2 fitness value, which considers the Pareto strength of the solution and its sparsity. Specifically, the Pareto strength consists of a comparison of the multiple objectives, while the sparsity of a solution is a measure that forces the even exploitation of the solution space (i.e., diversity). When the nondominated front exceeds the archive size, the truncation technique is applied, whereas if the archive is incomplete, dominated individuals with the best fitness are copied into it. To breed a new population, mating selection, crossover and mutation strategies are applied to preserve the Pareto dominance while guaranteeing a diverse set of solutions. In this framework, the objectives of the MOO can be represented by the following equations:

$$\min E.C.\ [kgCO_2eq] = \min \sum_i (Mass_i \times\ EC_{factor,i}) \tag{1}$$

$$\min E.U.I.\ [kWh/m^2/year] = \min \sum_r (CE_r + HE_r + LE_r + EE_r) \tag{2}$$

$$\max L_{flex}\ [m] = \min \left(-\sqrt{L_{gravity}^2 + L_{seismic}^2} \right) \tag{3}$$

where: *E.C.* is the total Embodied Carbon of the building as the sum of the embodied carbon of all the building's materials; *E.U.I.* is the End Use Intensity as the sum of the Cooling Energy demand *CE*, the Heating Energy demand *HE*, the Lighting Energy demand *LE*, and the Electric Equipment energy demand *EE* of every thermal zone *r* in the building, representing the total normalized thermal annual load; L_{flex} is a measure of the internal space flexibility expressed as the maximum free span between vertical structural members, with $L_{gravity}$ and $L_{seismic}$ being the span length in the gravity load resisting frame's direction and the seismic load resisting frame's direction, respectively. The minus sign in Eq. (3) is necessary because the optimization algorithm operates by minimizing objective functions. Therefore, to represent a quantity that should be maximized, the function is expressed with a negative sign, allowing the algorithm to seek the largest value by minimizing its negative. The maximum diagonal distance between two columns was selected as the flexibility metric because a structure with fewer internal obstructions allows for easier reconfiguration of the floor layout. A greater spacing between load bearing elements enables the creation of multiple room arrangements within the same floor area. On the other hand, shorter distances limit the design possibilities, often requiring smaller rooms to ensure that each column remains within the room boundaries. Although this specific metric has not appeared in previous studies, its physical meaning aligns well with flexibility indicators and adaptability criteria used in several works (e.g., Geraedts 2016; Cavalliere et al. 2019; Blok and Herwijnen 2006). Moreover, it is defined as a function of the post-tensioned span length and the gravity span length, which are two of the structural variables iteratively modified by the optimization algorithm, as described in the next paragraph. As a result, changes in *Lflex* also influence seismic performance and embodied carbon (the latter depending on the quantity of raw materials used), as well as energy performance through variations in the internal occupancy area and the window-to-wall ratio. Indeed, modifying the span length

also changes the façade composition, since the number and size of windows remain constant while the opaque wall area increases, resulting in a corresponding variation in the window-to-wall ratio. It is therefore clear how Eq. (3) represents a conflicting goal when compared to Eqs. (1) and (2), with the aim of extending the internal space as much as possible to create an adaptable building, while using as little material as possible and reducing the building energy demand. To reach these objectives, input parameters (called "genomes") are iteratively changed during the optimization process. In this study, the genomes are represented by geometric measures of the building configuration along with design targets, as illustrated in Table 1. To guarantee the feasibility of the investigated solutions, i.e., compliance with materials strength limits and the seismic demand, hard constraints are included in the MOO, expressed through Boolean true/false statements within the Grasshopper model. A penalty on the global ratio between re-centering and dissipative contribution in the post-tensioned frames is also given, meaning that all the solutions with a re-centering ratio lower than 1.15 are rejected from the evaluation.

- *Structural modelling and seismic analyses*. The seismic response of Pres-Lam frames is modelled through a lumped plasticity approach (Fig. 3a) implemented within an external Python script using Opensees software (McKenna 2011; Zhu et al. 2018). The frames and sections input data are stored in a JSON file and transferred from the Grasshopper model to the Python script. To simulate the behaviour of the hybrid sections, two rotational springs are inserted at the end sections of the structural members in the beam-column joint and column base. The first spring represents the energy dissipation of the mild-steel external damping devices through a Giuffrè-Menegotto-Pinto hysteresis rule; the second rotational spring simulates the post-tensioning cables with a multilinear elastic link. To model the joint panel deformation, a linear elastic link is used with the elastic stiffness derived from the formulations proposed by Pampanin et al. 2013 for both external and internal joints. The parameters related to the dissipaters and the post-tensioning tendons are obtained using the Monolithic Beam Analogy developed by Pampanin et al. 2001 and further adapted to Pres-Lam by Newcombe et al. 2008.

To assess the seismic performance of the Pres-Lam frames, a probabilistic approach is chosen by using fragility curves to obtain the Mean Annual Frequency of Exceed-

Table 1 List of optimization design variables and constraints

	Definition	Unit
Design variables	Pres-Lam beam height	mm
	Pres-Lam column height	mm
	Seismic frame span	m
	Gravity frame span	m
	DDBD target design drift	%
Constraints	Design check (Moment Capacity ≥ Acting Moment)	kNm
	Beam's deflection ≤ L/300	mm
	Column compressive stress ≤ material compressive strength	MPa
	Re-centering ratio (Re-centering moment / dissipative moment) ≥ 1.15	-
	SLS inter-storey drift ≤ SLS code-compliant target drift	%

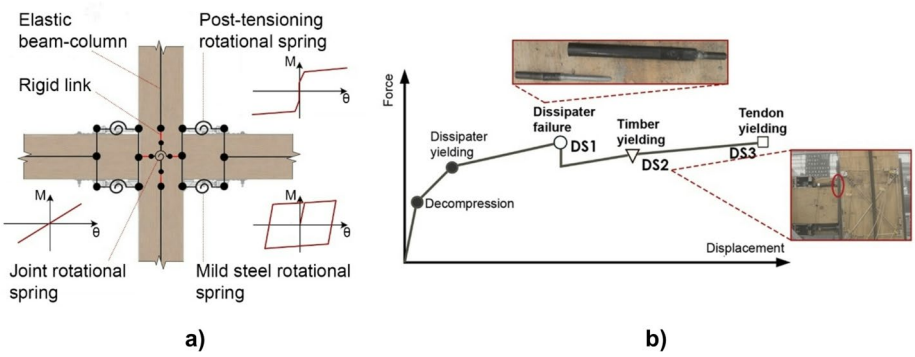

Fig. 3 **a** Lumped-plasticity modelling of a rocking-dissipative hybrid connection (beam-column joint), **b** Damage states of a Pres-Lam connection

ance (MAFE) related to various limit states. To develop the fragility curves, a non-linear time history analysis (NLTHA) approach is used implementing the Incremental Dynamic Analysis (IDA) methodology (Vamvatsikos and Cornell 2002). The procedure employs a suite of ground motions that are progressively increased until the onset of the desired limit state is achieved. In the framework, the suite of 44 ground motions (22 recordings times 2 directions) provided by FEMA P-695 (FEMA 2009) is used to perform the analysis. This set (listed in Appendix – Table A1) contains records selected from all large-magnitude events in the PEER NGA database (PEER 2006), in sufficient number to permit record-to-record variability. Once the set of Intensity Measure (IM) values associated with the occurrence of the considered limit states are collected, the cumulative distribution function of the probability of exceeding each limit state can be computed. The considered Limit States (or Damage States) for the Pres-Lam frames are the following (Fig. 3b): DS1 is the failure of the external dissipaters, represented by the gap opening that induces a 6% axial deformation in the fuse-shaped devices; DS2 is the limit state corresponding to the timber yielding in compression parallel-to-the-grain; DS3 is the yielding of the post-tensioning tendons in the beams.

The global onset of each DS is achieved once at least one section reaches the defined limit state. Since every section of the frame might reach the above-defined damage states for a different amount of gap opening, the Demand Capacity Ratio (DCR) is defined as the Engineering Demand Parameter (EDP) for the analysis, in place of the gap opening itself. The DCR is represented as the ratio between the maximum gap opening that occurred during the NLTHA ($D_{gap,\,j}$) and the gap opening corresponding to the onset of the considered damage state in the specific connection $C_{gap,\,j}(DS)$. Gap opening has been recognized as a reliable damage indicator for Pres-Lam rocking connections, instead of the conventional inter-storey drift ratio. This choice is supported by recent studies showing that using either indicator as an EDP yields comparable results (Matteoni et al. 2024). The global DCR is then computed as the maximum between all the connections n, defined as follows:

$$DCR_{DS} = max_j^n DCR_{DS,j} = max_j^n (D_{gap,j}/C_{gap,j}\,(DS)) \tag{4}$$

The considered Intensity Measure (IM) is the Spectral Acceleration at the first-mode period $S_a(T_1)$. Following the Performance-Based Earthquake Engineering (PBEE) principles, the Mean Annual Frequency of Exceedance (MAFE) of the limit states is computed integrating the fragility curves obtained from the IDA with the hazard curve relative to the building site and the building's first-mode period. To obtain the hazard curves, the analytical approach proposed by Vamvatsikos 2012 is used with a second-order hazard approximation. The MAFE is then defined by Eq. (5):

$$\lambda_{DS} = \int_0^{IM_{T_R^*}} P\left[DCR_{DS} \geq 1 | IM = x\right] \times \left| d\lambda_{IM}(x) \right| + 10^{-5} \tag{5}$$

Where a probability of occurrence of the damage state equal to 1 for return periods (T_R) higher than 10^5 is considered (Iervolino et al. 2018).

3 Application to a Pres-Lam case-study building

A three-storey office building is considered to validate the integrated parametric framework (Fig. 4a). The building features four 6-span post-tensioned timber (Pres-Lam) frames in the longitudinal (X) direction (Fig. 5), and four post-tensioned timber walls in the transversal (Y) direction as the lateral-load resisting systems, and an inter-storey height of 3.6 m. Simple 3-span moment-resisting timber frames carry the gravity loads in the Y direction across the building. The flooring system consists of timber-concrete composite (TCC) floors. This flooring system enables large spans by leveraging the combined strength of timber joists and a concrete slab and shows a better vibration performance when compared to the more traditional CLT floor for the same span length (Casagrande et al. 2018). As far as the envelope is concerned, CLT-based cladding panels with insulations are used in the X direction, connected to the post-tensioned frames by means of low-damage connections (Baird et al.

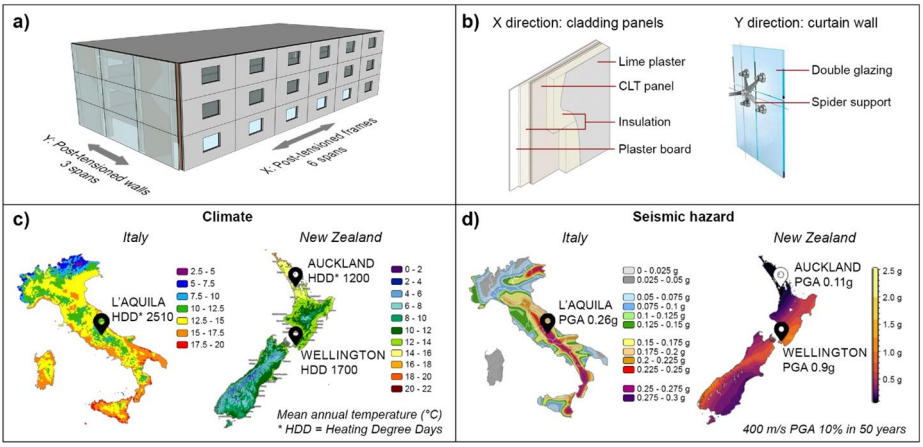

Fig. 4 **a** Pres-Lam case-study building and the lateral-load-resisting systems in the two directions, **b** the façade systems, **c** climate and **d** seismic properties of the three locations considered

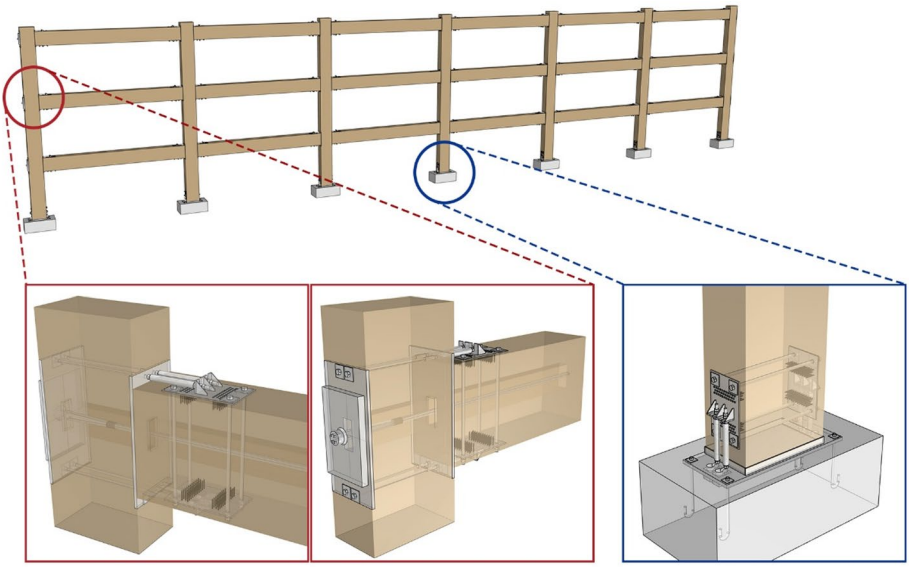

Fig. 5 Pres-Lam frame with details of beam-column and column-foundation connections

2013; Pampanin 2015). In the walls (Y) direction, the building is coated with a spider-glazing curtain wall (Fig. 4b).

Three different locations have been considered for the building (Fig. 4c, d): L'Aquila, situated in central Italy and known for its high seismic activity, with a value of Peak Ground Acceleration (PGA) of 0.26 g for a 10% Probability of Exceedance (PoE) in 50 years; Auckland and Wellington in New Zealand. Auckland is in the lowest seismic zone of the country with 0.11 g of PGA, while Wellington lies right on one of the nation's most active and powerful faults and is characterised by a PGA equal to 0.9 g due to near fault effects. The building is designed considering an Importance Level 3, a type C soil for both L'Aquila and Auckland, and a type B soil for Wellington, following the NTC 2018 (Ministero delle Infrastrutture e dei Trasporti 2018) and NZS 1170.5:2004 (Standard New Zealand 2004) for the definition of the response spectra in the two countries. It is worth noting that Importance Level 3, which corresponds to office buildings in the abovementioned codes, could also be adopted when applying the framework to residential buildings. Using a higher importance level than strictly required would be consistent with the Performance-Based Engineering philosophy of targeting higher damage-control performance levels by imposing greater seismic demand. In addition, this approach would facilitate potential future changes of use from residential to office occupancy.

The EPDs for the Life-Cycle Assessment have been chosen considering the two different countries of origin, and the weather data of the three cities are collected. In this regard, Auckland is characterised by an almost subtropical climate, with a small temperature variation across the year of about 10 °C and an average maximum temperature of around 25 °C; on the other hand, L'Aquila has a sub-continental climate, with an average minimum temperature slightly below 0 °C and the maximum still around 25 °C. Finally, the climate of

Wellington is characterised by strong winds, and overall dry and sunny conditions all over the year, being a temperate-oceanic climatic region (average annual temperature of 13 °C).

For the structural elements (beams and columns) of the post-tensioned frames, Laminated Veneer Lumber (LVL) has been chosen with a flexural strength of 44 MPa and a parallel-to-grain modulus of elasticity of 14,000 MPa for Italy (Steico 2017). Similarly, LVL13 has been used for New Zealand (modulus of elasticity of 13200 MPa and bending strength of 48 MPa, Nelson Pine 2016). The unbonded post-tensioning tendons are made of 7-wire strands, characterized by a yielding tensile strength of 1670 MPa, while the external mild-steel "Plug&Play" dissipaters features a yielding strength of 355 MPa. Internal steel rods are provided to reinforce the columns against crushing perpendicular-to-the-grain. The determination of both the quantity and sizes of the Plug&Play dissipaters, as well as the number of post-tensioned tendons, is carried out through the DDBD procedure outlined previously.

The Multi-Objective Optimization (MOO) and the seismic analyses are performed only for the Pres-Lam frames in the longitudinal direction, while the environmental and energy analyses are conducted on the whole building, considering both the structural and non-structural components described above. The "genomes" changed at each iteration by the evolutionary algorithm are the beams and columns section height of the post-tensioned frames, the Pres-Lam frames (longitudinal) span length, the gravity (transversal) frames span length, and the target design drift at the Ultimate Limit State (ULS) for the DDBD procedure. The target drift for the Serviceability Limit State (SLS) has been set equal to 0.5% for Italy and 0.3% for New Zealand, following the different seismic codes. Table 2 provides a summary of the optimization settings and parameters, the domain of the input parameters varied during the optimization process, and the energy parameters for the dynamic simulations. For standardization limits in the LVL production, the beams and columns width are fixed at 405 mm, made of nine 45 mm thick laminations glued together. Although no standardization has been used for the section height, it is worth noting that a second-level optimization should be carried out to reduce residual material in the manufacturing process.

Table 2 Multi-Objective optimization and analyses parameters for the three locations

	Parameter	L'Aquila	Auckland	Wellington
MOO settings	Elitism		0.5	
	Mutation rate		0.9	
	Crossover rate		0.8	
	Population size	50	50	30
	Generations until convergence	31	20	37
Genomes (min ÷ max)	Beam height (mm)		500 ÷ 900	
	Column height (mm)		500 ÷ 1000	
	Seismic span (m)		5 ÷ 10	
	Gravity span (m)		5 ÷ 10	
	Design drift (%)		1 ÷ 2	
Energy simulations	Cooling setpoint (°C)		24	
	Heating setpoint (°C)		21	
	Infiltration (m^3/s-m^2)		0.23e-03	
	Occupancy (people/m^2)		0.071	
	Lighting (W/m^2)		10	
	Equipment (W/m^2)		7.5	
	U value – X façade (W/m^2-K)		0.15	
	U value – Y façade (W/m^2-K)		2.22	

3.1 Optimization results

Two optimal solutions on the Pareto front have been selected for each case-study location (Fig. 6), namely the least and the most flexible one, in order to explore the most different building configurations and their performance. It is safe to say that all those solutions lying between the two selected are characterised by different trade-offs among the performance objectives. Therefore, examining the extremes can offer a meaningful overview of the results.

The input parameters of the selected optimal solutions and the corresponding objectives values generated by the MOO are listed in Table 3.

The algorithm was able to find those frame's section dimensions, and the number and diameters of external dissipaters, which can accommodate the different seismic demands at the three sites, while reducing at most the use of material and maximising the span length. Specifically, in the Wellington case study, the algorithm quickly identified a sufficient number of Pareto non-dominated solutions to populate the Elite space while preserving solution diversity throughout the convergence process. To accomplish this task, different values of design drift for the DDBD were chosen during the optimization process, with lower values usually corresponding to larger, thus less stiff, frames. An exception occurs in the case of Auckland, where the shorter and stiffer frame was designed for a lower drift than the longer one, even if the difference in span length is not as significant as for the other two locations. This is possibly due to the lower seismicity of the city, which allows for a wider choice of flexible building configurations and greater freedom in the design parameters. All the solutions found by the algorithm comply with the materials strength and deformation limits

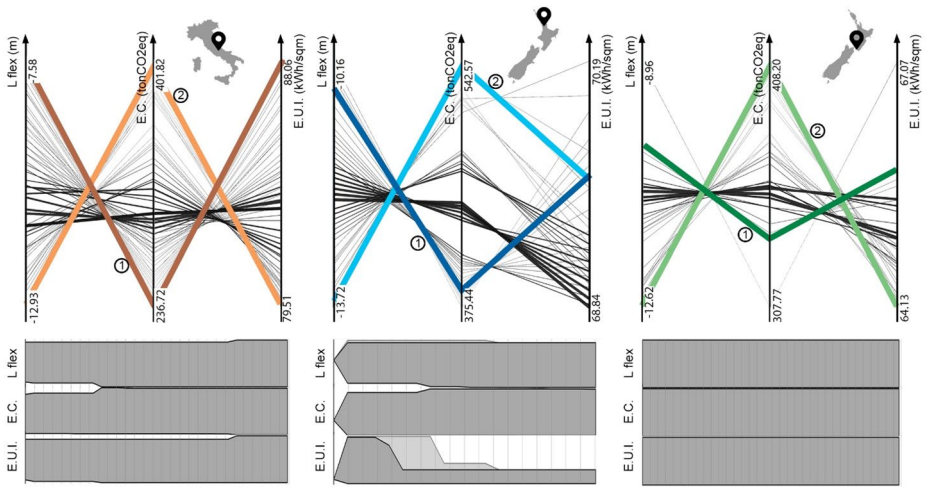

Fig. 6 On top, MOO solution space visualization and the selected optimal solutions (where solution 1 is the least flexible building configuration, and solution 2 the most flexible) for the three case-study locations: each solution is represented by a polyline whose vertices meet different objectives values (i.e., internal space flexibility L_{flex}, Embodied Carbon E.C., and End Use Intensity E.U.I.). At the bottom, convergence graphs for each objective function at the three different locations, showing the upper- and lower-bounds of the pareto-front (dark grey) and the Elite (light grey, background) throughout the generations (the bounds are normalized to an interval of [0;1]). A convergence graph entirely in dark grey indicates that the algorithm has identified a sufficiently large number of Pareto non-dominated solutions to fill the entire elite population

Table 3 Optimization design variables and objectives values of the selected optimal solutions for each building location

	L'Aquila		Auckland		Wellington	
	1st solution	2nd solution	1st solution	2nd solution	1st solution	2nd solution
Design drift (%)	1.9	1.5	1.6	2	1.8	1.5
Seismic span (m)	5.8	8.2	8.6	9.4	6.3	8.7
Gravity span (m)	5	10	6	10	8	9
Beam height[a] (mm)	610	900	520	640	660	880
Column height[a] (m)	520	710	880	690	720	1000
Number of dissipaters – beams[b]	2,2,2	3,2,2	2,2,2	2,2,2	2,2,2	2,2,2
Diameter of dissipaters (mm) – beams[b]	14,14,14	16,16,14	14,14,14	14,14,14	14,14,14	16,14,14
Number of PT tendons – beams[b]	4,3,2	6,5,2	3,2,1	3,3,2	4,3,2	4,3,2
Number of dissipaters – columns	3	3	2	2	2	2
Diameter of dissipater (mm) – columns	14	22	14	14	22	22
E.C. (tonCO_2eq)	237	402	384	540	335	408
E.U.I. (kWh/m^2/year)	88	79	70	70	66	64
Window-to-wall ratio (X direction)	0.2	0.11	0.13	0.12	0.18	0.13
Window-to-wall ratio (Y direction)	0.04	0.52	0.2	0.52	0.4	0.47

[a] *Beams and columns section width is fixed to 405 mm*

[b] *From level 1 to 3*

outlined in Table 1, as well as the minimum required re-centering ratio of 1.15. It is worth mentioning that the variation in section dimensions, number of post-tensioning tendons, and overall frames stiffness between the case studies in Italy and New Zealand is also influenced by the different target drifts at the Serviceability Limit State (SLS) for the two countries. This sizing of the timber frame's elements is in fact governed by this limit state, as previously explained.

An overview of the selected solutions for each site with their seismic, energy and environmental performance is provided in Fig. 7. As expected, the smaller buildings are characterised by lower values of embodied carbon (Table 3), which becomes almost twice when doubling the frames spans. It is worth noting, however, that the greatest amount of materials-related carbon emissions is due to the non-structural components for all the building configurations, mainly influenced by the use of glass for the curtain walls in the Y direction. This outcome confirms the advantages of using timber in construction, thanks to its low environmental impact. Additional insights on the environmental performance of the buildings can be gained by conducting a comprehensive whole life-cycle assessment, whose results will be later presented.

As far as the energy consumption is concerned, variations are due to the distinct climatic conditions at the three sites, as will be subsequentially discussed. At the same time, the different building volumetric configurations and the window-to-wall ratios deriving from the optimization process play a fundamental role in determining the energy required to maintain a comfortable indoor environment. The results of the dynamic energy simulations in terms of End Use Intensity (E.U.I.) will be included in the cradle-to-grave LCA as part of the operational phase module (operational energy use).

The Mean Annual Frequency of Exceedance (MAFE) of the Damage States (DS) associated with Pres-Lam frames was used to assess and compare the seismic performance of the

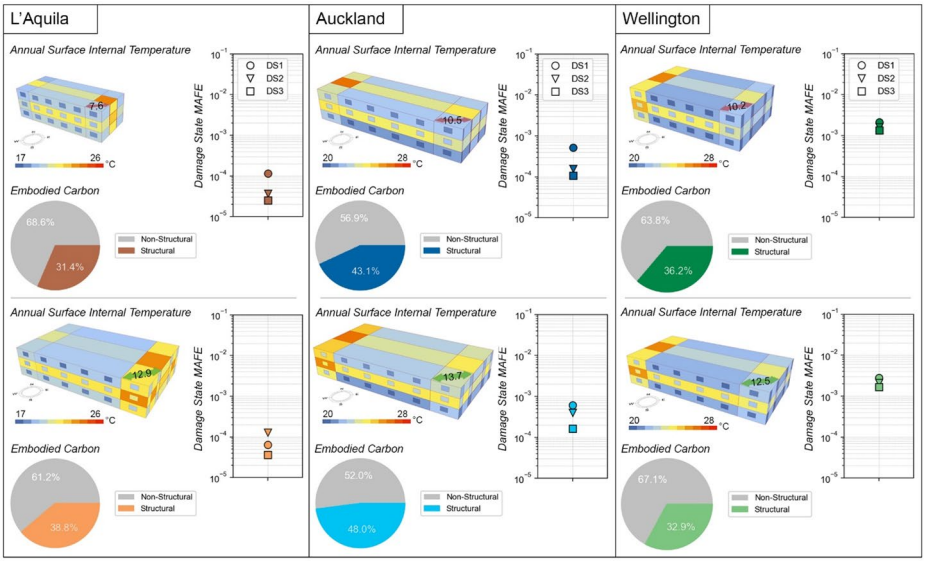

Fig. 7 Summary of the two chosen optimal solutions (top row: least flexible, bottom row most flexible) for each building location: a representation of their average surface internal temperature, the relative Embodied Carbon of their structural and non-structural components, and their seismic performance as the Mean Annual Frequency of Exceedance (MAFE) of the damage states

selected solutions. The MAFE is obtained by integrating the damage state fragility curves with the hazard curve corresponding to the site and to the first-mode period of the buildings. The results are influenced by the different frame configurations generated through the optimization process, the design parameters adopted as inputs (e.g., target/design drift), and the seismic hazard specific to each city. Further considerations are provided in the following paragraph.

3.2 Seismic performance

Lateral loads are resisted by four post-tensioned frames in the longitudinal (X) direction for L'Aquila and Wellington case studies, while only two seismic-resistant Pres-Lam frames are sufficient in the Auckland's buildings due to the relatively low seismic demand. The Pres-Lam frame's damage states MAFE of each solution are listed in Table 4. In the case of L'Aquila, the increase of building spans for both seismic and gravity frames in the second building configuration comes with the insurgence of Damage State 2 (i.e., timber yielding in compression) before Damage State 1 (i.e., failure of external dissipaters). This is due to the higher axial load in the sections, especially at the base of the columns. Despite that, the values of MAFE can be considered relatively low, with Damage State 3 (i.e., yielding of the post-tensioning tendons) close to the value of 10^{-5}, which corresponds to ground-motions with a return period TR = 100,000 years. On the contrary, both Auckland and Wellington case studies show the expected hierarchy of limit states for Pres-Lam hybrid connections. This might be attributed to the lower acceptable drift value at the SLS, which results in frame's elements dimensions that effectively prevent the onset of the timber yielding's dam-

Table 4 Mean annual frequency of exceedance (MAFE) of the considered damage States (DS) for the chosen optimal solutions

Location	Solution	DS1	DS2	DS3
L'Aquila	1st	1.15e-04	3.71e-05	2.54e-05
	2nd	6.4e-05	1.3e-04	3.63e-05
Auckland	1st	5.2e-04	1.58e-04	1.07e-04
	2nd	6.1e-04	3.98e-04	1.63e-04
Wellington	1st	2.13e-03	1.61e-03	1.34e-03
	2nd	2.8e-03	2.13e-03	1.67e-03

age state before the dissipaters failure. However, both New Zealand case studies exhibit higher values of MAFE for each DS compared to the buildings in L'Aquila, even in the context of Auckland's lower seismic hazard. This is possibly due to the optimization of the post-tensioned frames to meet design requirements with as little material as possible, at the expense of a worse (yet still acceptable) seismic performance. It is also noteworthy that the post-tensioned frames under examination are herein exclusively designed to withstand lateral loads.

Figure 8 shows the damage state fragility curves (top row) of the Pres-Lam frames for the chosen optimal solutions, derived from Incremental Dynamic Analysis (IDA), and subsequentially integrated with the site's hazard curve relative to the building first-mode period (T1) to obtain the MAFE.

The fragility functions parameters are listed in Table 5. The fragility curves of Auckland's case studies are characterised by the lowest values of the median, confirming their previously mentioned higher vulnerability to damage. Despite being the less hazardous site, the higher probability of exceeding the damage states leads to higher MAFE, as shown also by the integrand functions (Fig. 8, bottom row). On the other hand, Wellington and L'Aquila case studies show comparable values of the median, but the significantly higher seismic hazard of Wellington results in equally higher MAFE compared to the Italian site. In all the cases, the most flexible solutions (i.e., the second solutions) have a probability of exceeding DS2 closer to DS1. Reinforcement strategies are then suggested in these buildings to prevent the insurgence of this permanent damage state prior to the failure of the external dissipaters, which can instead be classified as a serviceability limit state due to their replaceability. Overall, it is noteworthy that employing the Multi-Objective Optimization design approach yields satisfactory results when compared to conventional iterative-intuitive design methods.

3.3 Energy performance

The results of dynamic energy simulations are expressed in the form of End Use Intensity, representing the energy required for cooling, heating, lighting, and operating electric equipment. Of these end-use, the last two are fixed for all the case studies, as expressed in Table 2, while the first two highly depend on the climatic zone where the building is located, as well as the building configuration. In this study, the window-to-wall ratio also significantly impact energy consumption, by implicitly changing during the optimization process when varying the frames span length. As already anticipated, the high temperature range of L'Aquila (Fig. 9) makes necessary the use of HVAC to maintain internal comfort. This explains the higher difference in EUI value between the two optimal solutions in this city when compared to the values observed in both Auckland and Wellington. This difference is

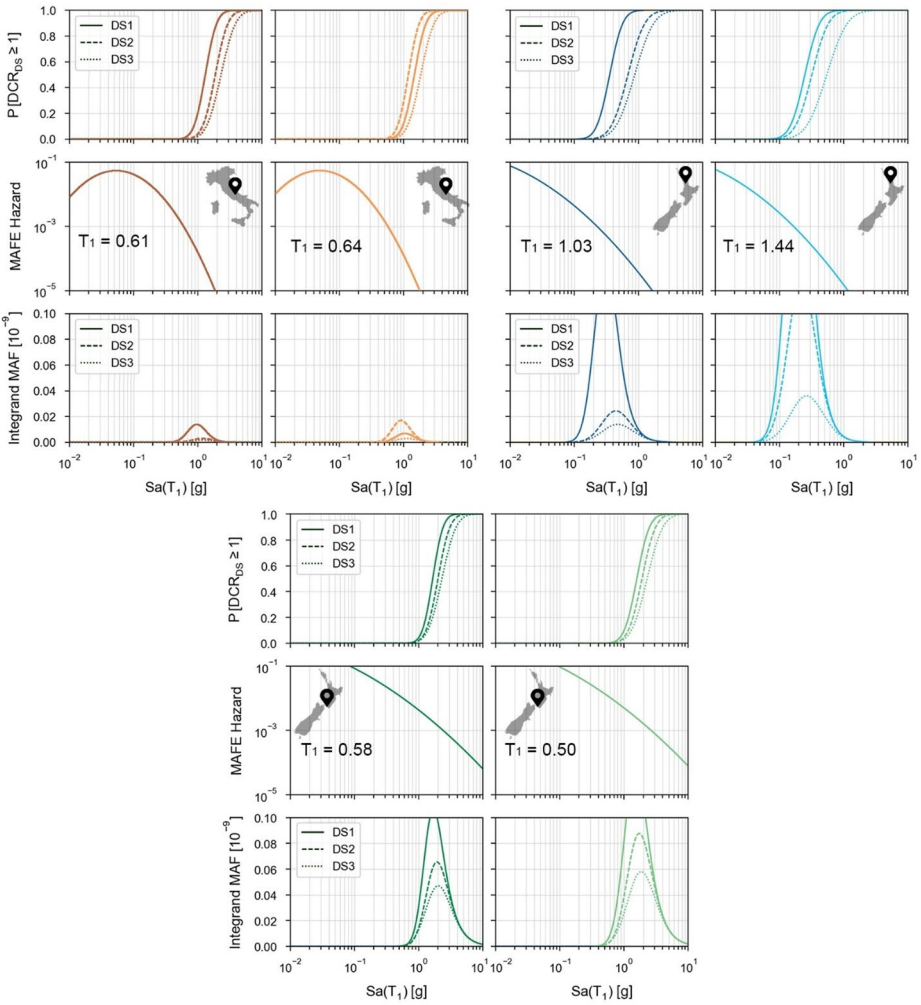

Fig. 8 Damage state fragility in logarithmic scale (top), site hazard curve fitted using the second order approximation (Vamvatsikos 2012) for the specific T1 (centre), and Mean Annual Frequency (MAF) integrand function scaled by a factor of 10^9 (bottom) for each optimal solution

Table 5 Median θ and standard deviation β of the damage state fragility functions

Location	Solution	DS1		DS2		DS3	
		θ	β	θ	β	θ	β
L'Aquila	1st	1.31	0.32	2.30	0.41	1.88	0.36
	2nd	1.47	0.33	1.85	0.38	1.19	0.31
Auckland	1st	0.36	0.37	0.69	0.48	0.88	0.53
	2nd	0.25	0.42	0.32	0.47	0.54	0.58
Wellington	1st	1.66	0.29	2.31	0.39	2.00	0.34
	2nd	1.59	0.35	2.30	0.44	1.91	0.38

also due to the lower window-to-wall ratio in the 2nd (i.e., most flexible) building configuration, which helps to reduce the dispersion through the glass components of the building envelope, therefore reducing the energy use intensity.

For the two cities in New Zealand, the difference in EUI between the smaller and larger buildings is almost negligible due to the milder climatic conditions, which generally result in lower energy consumption across all building sizes with respect to L'Aquila. The milder climate of Auckland and Wellington allows to meet internal thermal comfort almost exclusively with natural ventilation, significantly reducing the energy needed for heating and cooling, which represents the main contribution to energy consumption throughout the year (Fig. 10). This is particularly true in the case of Wellington, characterised by the lowest energy intensity values, which are not really influenced by difference in the window-to-wall ratio.

To assess the influence of HVAC modelling on the energy consumption results, a sensitivity analysis was conducted by modifying the HVAC systems used in Ladybug's Honeybee energy model from the Ideal Loads System adopted during the optimization process. Specifically, two alternative systems were examined: an all-air Variable Air Volume (VAV) HVAC system that provides both ventilation and heating/cooling using the same air stream; and a Dedicated Outdoor Air System (DOAS), which separates minimum ventilation supply from heating and cooling needs by delivering air at a neutral temperature and using additional zone equipment (e.g., fan coil units) to meet thermal demands. The sensitivity analysis has been carried out just for the Pareto-optimal selected solution, and its results are listed in Table 6 in terms of End Use Intensity (kWh/sqm/year).

When comparing the results of an Ideal Air Loads system to a real detailed HVAC system it is expected that annual energy use increases. Ideal Air Loads assumes perfect distribution, infinite equipment efficiency, and no fan or ventilation energy. In contrast, a real HVAC system introduces several additional energy demands, including fan electricity, coil inefficiencies, minimum airflow requirements, reheat, and conditioning of outdoor ventilation air. These factors typically raise the total energy use significantly. However, it is worth noting that the E.U.I. ranking across the optimal solutions for the three case-study locations remain

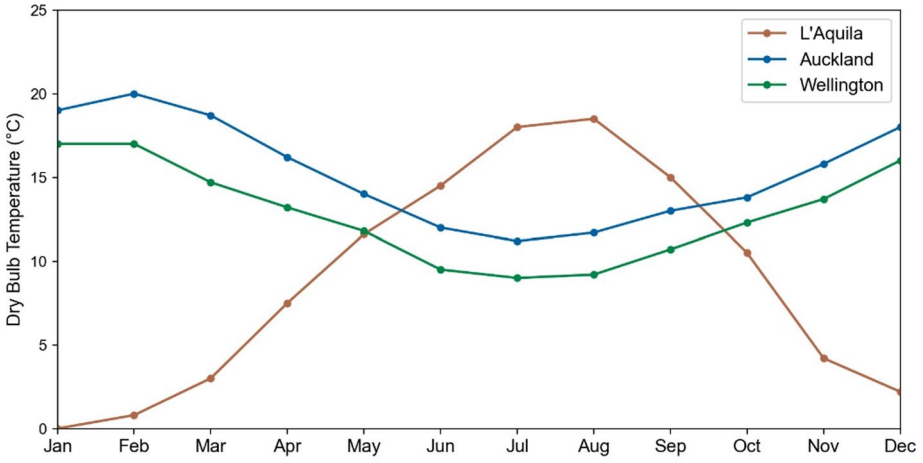

Fig. 9 Average temperature over the year for the three cities

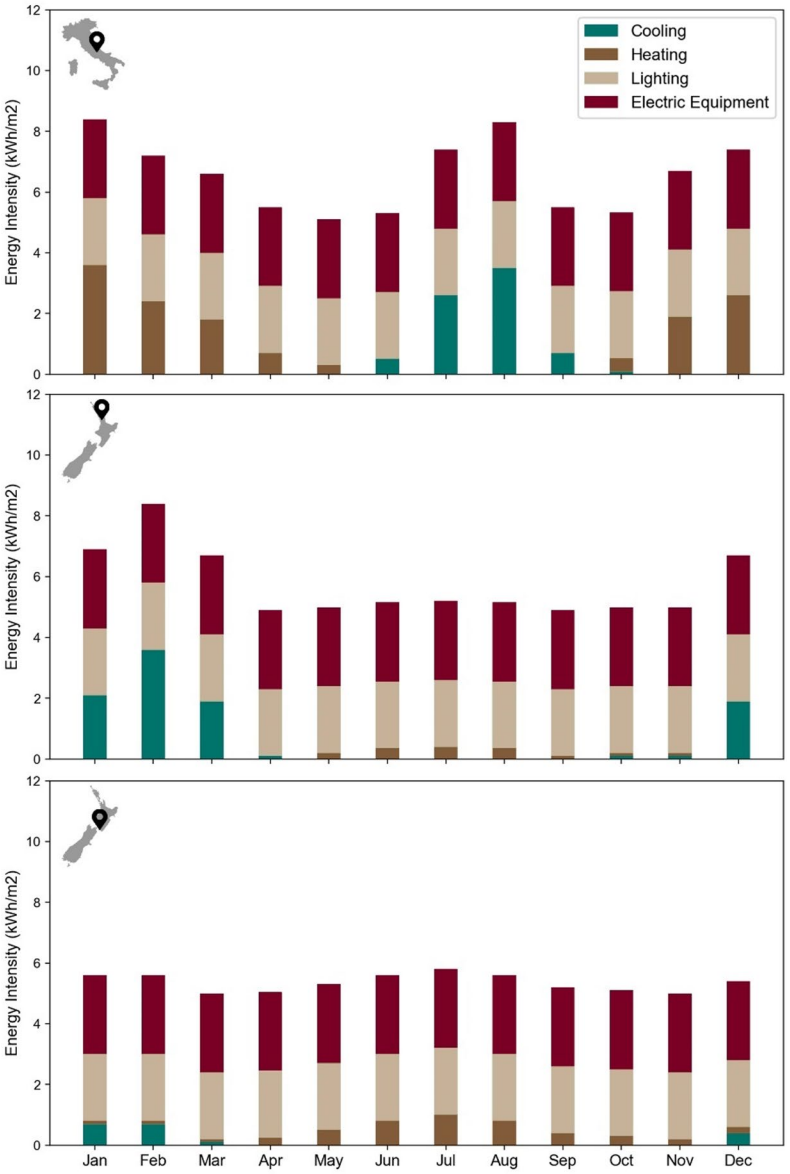

Fig. 10 Energy Intensity: energy usage over the year for the first building configuration of each location, subdivided into the main end-use

consistent when switching from the idealized, loss-free HVAC system to a more realistic one, confirming the robustness of the optimization outcomes.

Both the energy consumption of L'Aquila and those of Auckland and Wellington optimized case studies are significantly lower than the average energy intensity of office buildings in Italy and New Zealand, which are, respectively, around 290 kWh/m2 per year (ENEA 2023) and 200 kWh/m2-year (Amitrano et al. 2014).

Table 6 Energy consumption results for the selected Pareto-optimal solutions when varying the HVAC system

Location	Solution	End Use Intensity (kWh/sqm/year)		
		Ideal HVAC	All-air HVAC	DOAS HVAC
L'Aquila	1st	88	114	119
	2nd	79	107	111
Auckland	1st	70	96	96
	2nd	70	98	98
Wellington	1st	66	95	95
	2nd	64	90	90

3.4 Environmental impact

While the solely embodied carbon has been considered as an objective for the MOO, a whole Life-Cycle Assessment is performed using the One Click LCA cloud software to better analyse the environmental impact of the selected optimal solutions related to each life-cycle stage from cradle-to-grave. All the stages covered by the BSI EN 15,978 Standard (British Standard Institute 2011) have been considered. The Operational energy use phase (B6) is obtained from the energy analyses described in the previous paragraph. It is worth saying that the maintenance and replacement stages (B2-B5) consider only the impacts from restoring the building products after they reach the end of their service life within the 50-year LCA reference time of the building, without taking into account the rehabilitation required following a potential hazard(Menna et al. 2013; FEMA 2018; Belleri and Marini 2016). However, we might safely assume that the contribution of that stage would be relatively low, because of the use of a low-damage structural system such as the Pres-Lam technology (Bianchi et al. 2023). Regarding the End-of-Life (EoL) phase (C), this study examined the possibility of reusing low-damage timber elements and recycling steel and glass components, (e.g., curtain walls). These EoL scenarios are addressed just as a reduction in CO2 emissions in the C stages, without considering the consequential cutting of the required raw-materials (stages A1-A3) in the following product cycle, as a more circular approach would have required.

Figure 11 shows the LCA results in terms of Greenhouse Gas (GHG) emissions of all the optimal solutions. It is evident how the operational energy use (B6 stage) represents the primary source of GHG emissions (Fig. 11a), followed by the materials production phase (Fig. 11b). Specifically, the most flexible (i.e., larger) case-study building located in L'Aquila is the one with the highest energy-related GHG emissions. This might also be due to the higher environmental impact of the Italian national electricity grid compared to the New Zealand one, which accounts for 0.49 kgCO2eq/kWh and 0.21 kgCO2eq/kWh respectively (source: One Click LCA database). As expected, the material-related GHG emissions (A1-A3 stages) are proportional to the buildings' dimensions, with the most flexible solutions having greater values in each location. Both the energy consumption and the material production phases make these solutions the worst performing in terms of environmental impact, as also highlighted in Table 7. However, if the adaptability of the building is considered, the possibility to accommodate changes in use can be potentially extend the life-cycle, thus reducing the nominal environmental footprint per year and avoiding those related to the construction of a new building. The emissions coming from the other LCA stages are significantly lower, thanks to the use of the low-damage and pre-fabricated Pres-Lam structural system.

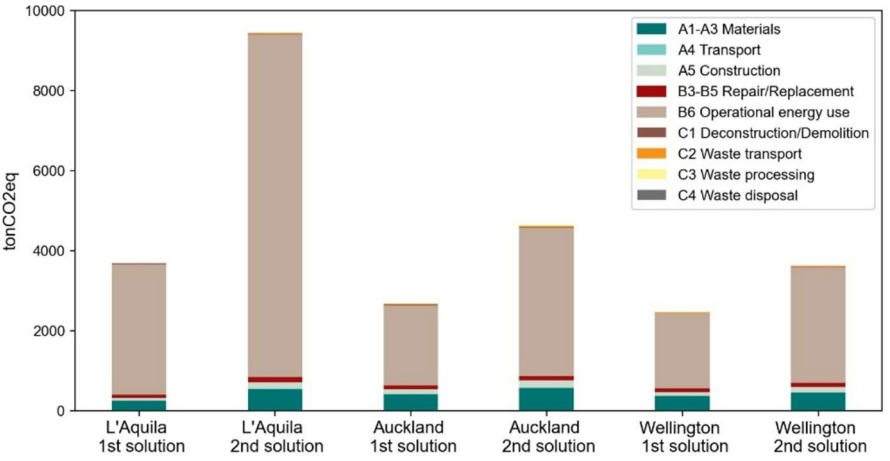

a)

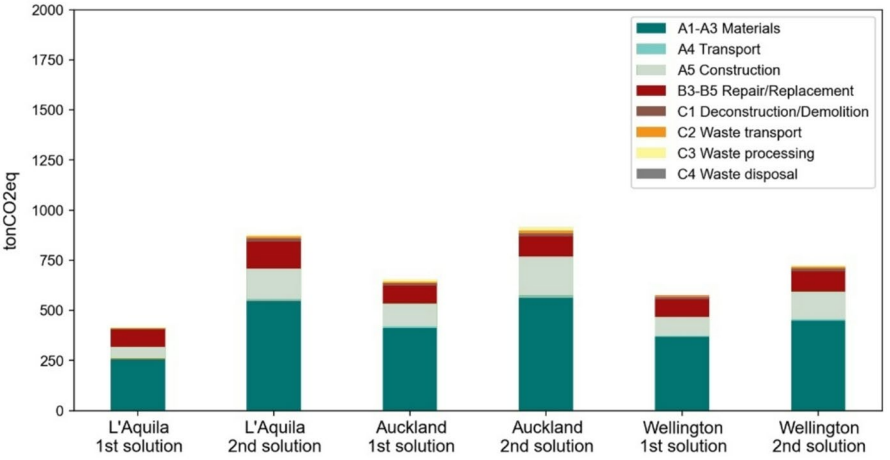

b)

Fig. 11 **a** Whole Life-Cycle Assessment results: Greenhouse Gas (GHG) emissions of the chosen optimal solutions over the stages of their life-cycle, **b** Same results when the Operational energy use (B6) stage is excluded

Table 7 Total carbon dioxide equivalent emissions divided by the assessment period (50 years) and the gross internal floor area of each Building

Location	Solution	Gross Internal Floor Area (m^2)	CO2 equivalent emissions ($kgCO2eq/m^2/year$)
L'Aquila	1st	1539	3.96
	2nd	4428	4.45
Auckland	1st	2786	1.69
	2nd	5076	1.78
Wellington	1st	2722	1.59
	2nd	4228	1.68

Overall, the MOO framework effectively identified sustainable, high performance building solutions, showcasing Pres-Lam potential to reduce both environmental footprints and post-earthquake damage. It is worth noting that many other configurations could achieve these goals, as only the extremes of the Pareto front were presented.

4 Conclusions

This study presented an integrated parametric framework for the multi-performance optimal design and evaluation of flexible low-damage post-tensioned laminated timber (Pres-Lam) buildings. The framework was developed within the Grasshopper environment, allowing to follow an automated Direct Displacement-Based Design procedure, and simultaneously perform environmental Life-Cycle Assessment (LCA) and dynamic energy simulations. To address and evaluate the trade-off between building performances, a Multi-Objective Optimization (MOO) is implemented through the SPEA-2 genetic algorithm. Design variables are iteratively changed to find optimal building configurations with the lowest embodied carbon and operational energy use, and the most flexible internal space. To assess the seismic performance of the solutions, Incremental Dynamic Analyses are performed to derive damage-state fragility curves of the Pres-Lam frames.

The framework is applied to a three-storey case-study building located in L'Aquila (Italy), Auckland (New Zealand), and Wellington (New Zealand). The different climatic characteristics of these three locations are exploited to get insights into the energy performance of the selected optimal Pres-Lam buildings, while the highly different seismic hazard curves are used to calculate the Mean Annual Frequency of Exceedance (MAFE) of the damage states.

The application of the framework shows how such an integrated approach can capture results that might not be self-explanatory, and confirm the great potential of using the MOO in the early building design stage. The significant possibilities opened up by using the Pres-Lam technologies are also highlighted. This low-damage and low-carbon structural system allows for the reduction of carbon emissions while delivering superior seismic performance when compared to more traditional systems. The definition of adaptive buildings is also possible, without compromising the construction efficiency and safety. By reducing the high computational demands and narrow disciplinary focus of current practices, the framework enables the identification of holistic optimal design solutions while still preserving engineering judgment in the decision-making process and including architectural considerations into the multi-performance design/assessment, acknowledging the critical role of adaptability and flexibility in fostering resilient design.

The research work can be further improved and extended including the expected post-earthquake losses as an additional decision variable/design objective, also including their environmental impact in the LCA analysis. Specifically, a probabilistic component-based approach might be implemented to obtain both the Expected Annual Losses (EALs) and the Expected Carbon Losses (ECLs). The second should enter within the LCA procedure as the rehabilitation stage, while the first might be included in a LCC analysis to evaluate the economic and environmental savings resulting from using a low-carbon and low-damage structural system. Both might represent additional decision-variables in the developed optimization framework, to propose a fully comprehensive multi-performance design framework for sustainable and resilient buildings. A more refined optimization might also be implemented, by using a different genetic algorithm, defining a more in-depth methodology and design variables to assess the adaptive capacity of buildings, and including manufacturers specifications in the elements sections optimization. Finally, by further enhancing the computational efficiency, the framework could be developed into a practical design tool or software plug-in for real-world engineering and architectural projects.

Appendix

Table A1 Summary of earthquake events and recording station data for the record set (from PEER NGA database)

ID No.	Earthquake			Recording Station	
	M	Year	Name	Name	Owner
1	6.7	1994	Northridge	Beverly Hills - Mulhol	USC
2	6.7	1994	Northridge	Canyon Country-WLC	USC
3	7.1	1999	Duzce, Turkey	Bolu	ERD
4	7.1	1999	Hector Mine	Hector	SCSN
5	6.5	1979	Imperial Valley	Delta	UNAMUCSD
6	6.5	1979	Imperial Valley	El Centro Array #11	USGS
7	6.9	1995	Kobe, Japan	Nishi-Akashi	CUE
8	6.9	1995	Kobe, Japan	Shin-Osaka	CUE
9	7.5	1999	Kocaeli, Turkey	Duzce	ERD
10	7.5	1999	Kocaeli, Turkey	Arcelik	KOERI
11	7.3	1992	Landers	Yermo Fire Station	CDMG
12	7.3	1992	Landers	Coolwater	SCE
13	6.9	1989	Loma Prieta	Capitola	CDMG
14	6.9	1989	Loma Prieta	Gilroy Array #3	CDMG
15	7.4	1990	Manjil, Iran	Abbar	BHRC
16	6.5	1987	Superstition Hills	El Centro Imp. Co.	CDMG
17	6.5	1987	Superstition Hills	Poe Road (temp)	USGS
18	7	1992	Cape Mendocino	Rio Dell Overpass	CDMG
19	7.6	1999	Chi-Chi, Taiwan	CHY101	CWB
20	7.6	1999	Chi-Chi, Taiwan	TCU045	CWB
21	6.6	1971	San Fernando	LA - Hollywood Stor	CDMG
22	6.5	1976	Friuli, Italy	Tolmezzo	-

Acknowledgements This work was supported by MUR and ESF REACT-EU from the resources of the National Operational Programme (PON) - Research and Innovation 2014–2020 (D.M 1061/2021) for the Doctoral scholarship of Giada Formichetti. The authors also acknowledge the funding provided by the Horizon Europe MULTICARE project (Grant No. 101123467), and the PRIN project QuakeSAFE-GreenSHIELD (Prot. 2022W934KH).

Author contribution Giada Formichetti: Conceptualization, Investigation, Methodology, Formal analysis, Writing – Original Draft, Visualization, Funding acquisition; Giuseppe Loporcaro: Conceptualization, Supervision, Writing – Review & Editing; Stefano Pampanin: Conceptualization, Supervision, Writing – Review & Editing, Funding acquisition.

Funding Open access funding provided by Università degli Studi di Roma La Sapienza within the CRUI-CARE Agreement. This work was supported by MUR and ESF REACT-EU from the resources of the National Operational Programme (PON) - Research and Innovation 2014–2020 (D.M 1061/2021) for the Doctoral scholarship of Giada Formichetti. The authors also received funding by the Horizon Europe MULTICARE project (Grant No. 101123467), and the PRIN project QuakeSAFE-GreenSHIELD (Prot. 2022W934KH).

Data availability The datasets generated during and/or analysed during the current study are available from the corresponding author on reasonable request.

Declarations

Competing interest The authors declare that they have no known competing financial interests or personal relationships that could have appeared to influence the work reported in this paper.

References

Amitrano L, Isaacs N, Saville-Smith K, Donn M, Camilleri M, Pollard A et al (2014) Building energy enduse study (BEES) - Part 1: final report. BRANZ study report 297/1. Judgeford, New Zealand

Apellániz D, Pasanen P, Gengnagel C (2021) A holistic and parametric approach for life cycle assessment in the early design stages. 12th SimAUD Symposium

Baird A, Palermo A, Pampanin S (2013) Controlling seismic response using passive energy dissipating cladding connections. NZSEE Conference. Wellington, New Zealand

Belleri A, Marini A (2016) Does seismic risk affect the environmental impact of existing buildings? Energy Build 110:149–158. https://doi.org/10.1016/j.enbuild.2015.10.048

Bianchi S, Ciurlanti J, Overend M, Pampanin S (2022) A probabilistic-based framework for the integrated assessment of seismic and energy economic losses of buildings. Eng Struct 269:114852. https://doi.org/10.1016/j.engstruct.2022.114852

Bianchi S, Ciurlanti J, Overend M, Pampanin S (2023) Low-carbon & Low-damage technologies for improving the resilience of buildings. SECED Conference. Cambridge, UK

Blok R, Van Herwijnen F (2006) Quantifying structural flexibility for performance based life cycle design of buildings. International Conference On Adaptable Building Structures, Eindhoven, The Netherlands

British Standard Institute (2011) EN 15978. Sustainability of construction works - assessment of environmental performance of buildings - calculation method. London, UK

Brown NC, Mueller CT (2016) Design for structural and energy performance of long span buildings using geometric multi-objective optimization. Energy Build 127:748–761. https://doi.org/10.1016/j.enbuild.2016.05.090

Casagrande D, Giongo I, Pederzolli F, Franciosi A, Piazza M (2018) Analytical, numerical and experimental assessment of vibration performance in timber floors. Eng Struct 168:748–758
Cavalliere C, Dell'Osso GR, Favia F, Lovicario M (2019) BIM-based assessment metrics for the functional flexibility of Building designs. Autom Constr 107:102925
ENEA (2023) Rapporto annuale efficienza energetica 2023 (italian). Agenzia nazionale per Le Nuove tecnologie, l'energia e Lo sviluppo economico sostenibile. Rome, Italy
Federal Emergency Management Agency (FEMA) (2018) FEMA P-695 - Quantification of building seismic performance factors. Washington, DC.Federal Emergency Management Agency (FEMA) FEMA-P-58-4 - Seismic Performance Assessment of Buildings, Volume 4 - Methodology for Assessing Environmental Impacts. Washington, DC
Geraedts R (2016) FLEX 4.0, a practical instrument to assess the adaptive capacity of buildings. Energy Procedia 96:568–579
Granello G, Palermo A, Pampanin S, Pei S, Van de Lindt J (2020) Pres-Lam buildings: State-of-the-Art. J Struct Eng 146. https://doi.org/10.1061/(ASCE)ST.1943-541X.0002603
Holden T, Devereux C, Haydon S, Buchanan A, Pampanin S (2016) NMIT arts & media Building—Innovative structural design of a three storey post-tensioned timber Building. Case Stud Struct Eng 6:76–83
Holland JH (1975) Adaptation in natural and artificial systems. University of Michigan Press, Ann Arbor, Michigan
Iervolino I, Spillatura A, Bazzurro P (2018) Seismic reliability of Code-Conforming Italian buildings. J Earthq Eng 22:5–27. https://doi.org/10.1080/13632469.2018.1540372
International Energy Agency (IEA) (2021) Global status report for buildings and construction 2021. UN Environment and International Energy Agency, Paris, France
International Standards Organization (ISO) (2006a) ISO 14040. Environmental Management - Life cycle Assessment - Principles and framework. Geneva, Switzerland
International Standards Organization (ISO) (2006b) ISO 14044. Environmental Management – Life Cycle Assessment - Requirements and Guidelines. Geneva, Switzerland; 2006
Iqbal A, Pampanin S, Palermo A, Buchanan AH Seismic Performance of Full-Scale Post-Tensioned Timber Beam-Column Joints. 11th WCTE, Conference (2010) Riva del Garda, Italy
Konak A, Coit DW, Smith AE (2006) Multi-objective optimization using genetic algorithms: A tutorial. Reliab Eng Syst Saf 91:992–1007. https://doi.org/10.1016/j.ress.2005.11.018
Matteoni M, Ciurlanti J, Bianchi S, Pampanin S (2024) Fragility functions for low-damage post-tensioned timber frames. Earthq Eng Struct Dyn 53:4741–4762
McKenna F (2011) OpenSees: A framework for earthquake engineering simulation. Comput Sci Eng 13:58–66
McNeel R (2010) Grasshopper - Generative Modeling with Rhino. McNeel, Seattle, North America
Menna C, Asprone D, Jalayer F, Prota A, Manfredi G (2013) Assessment of ecological sustainability of a Building subjected to potential seismic events during its lifetime. Int J LCA 18:504–515. https://doi.org/10.1007/s11367-012-0477-9
Ministero delle Infrastrutture e dei Trasporti (2018) NTC 2018 - D.M. del Ministero delle Infrastrutture e dei trasporti del 17/01/2018 - Aggiornamento delle Norme Tecniche per le Costruzioni (italian). Rome, Italy
Moroder D, Smith T, Dunbar A, Pampanin S, Buchanan A (2018) Seismic testing of posttensioned Pres-Lam core walls using cross laminated timber. Eng Struct 167:639–654. https://doi.org/10.1016/j.engstruct.2018.02.075
Mueller CT, Ochsendorf JA (2015) Combining structural performance and designer preferences inevolutionary design space exploration. Autom Constr 52:70–82. https://doi.org/10.1016/j.autcon.2015.02.011
Nelson Pine (2016) Nelson pine LVL - Specific engineering design guide. Nelson, New Zealand
Newcombe MP, Pampanin S, Buchanan AH (2010) Experimental Testing of a Two-Storey Post-Tensioned Timber Building. 9USN/10CCEE Conference. Toronto, Canada
Newcombe MP, Pampanin S, Buchanan A, Palermo A (2008) Section analysis and Cyclic behavior of Post-Tensioned jointed ductile connections for Multi-Story timber buildings. J Earthq Eng 12:83–110. https://doi.org/10.1080/13632460801925632
New Zealand Concrete Society (NZCS) (2010) PRESSS design handbook. Wellington, New Zealand
Palermo A, Pampanin S, Buchanan A (2006) Experimental investigations on LVL seismic resistant wall and frame subassemblies. 1st ECEES Conference. Geneva, Italy
Palermo A, Pampanin S, Buchanan A, Newcombe M (2005) Seismic design of multi-storey buildings using laminated veneer lumber (LVL). NZSEE Conference. Taupo, New Zealand
Pampanin S (2005) Emerging solutions for high seismic performance of Precast/Prestressed concrete buildings. J Adv Concr Technol 3(2):202–223. https://doi.org/10.3151/jact.3.207

Pampanin S (2007) Developments in seismic design and retrofit of structures: modern technology built on the ancients' wisdom. Hazards and the built environment: attaining built-in resilience 400, Chap. 6. Taylor and Francis, London, pp 96–123

Pampanin S (2012) Reality-check and renewed challenges in earthquake engineering: implementing low-damage systems–from theory to practice. Bull NZ Soc Earthq Eng 45(4):137–160. https://doi.org/10.5459/bnzsee.45.4.137-160

Pampanin S (2015) Towards the ultimate earthquake-proof building: development of an integrated low-damage system. Persp Eur Earthq Eng Seismolog 2:321–358

Pampanin S, Christopoulos C, Priestley MJN (2002) Residual deformations in the Performance-Based seismic assessment of frame systems. Res Rep ROSE 226

Pampanin S, Ciurlanti J, Bianchi S, Perrone D, Palmieri M, Grant D, Granello G, Palermo A, Filiatrault A, Stojadinovic B, Correia AA (2020) Enhancing seismic safety and reducing seismic lossess: overview and preliminary results or SERA project – 3D shaking table tests on an integrated low-damage Building system. 17th WCEE. Sendai, Japan

Pampanin S, Palermo A, Buchanan AH (2013) Design guide Australia and new Zealand - Post-Tensioned timber buildings. Structural Timber Innovation Company (STIC), Christchurch, New Zealand

Pampanin S, Priestley MN, Sritharan S (2001) Analytical modelling of the seismic behaviour of precast concrete frames designed with ductile connections. J Earthq Eng 5:329–367

PEER (2006) PEER NGA Database. Pacific Earthquake Engineering Research Center, University of California, Berkeley, California

Priestley MN (1991) Overview of PRESSS research program. PCI J 36(4):50–57

Priestley MN (2002) Direct displacement-based design of precast/prestressed concrete buildings. PCI J 47(6):66–79. https://doi.org/10.15554/pcij.11012002.66.79

Priestley MN, Calvi GM, Kowalsky MJ (2007) Displacement-Based seismic design of structures. Earthq Spectra 24(2):555–557

Priestley MN, Sritharan S, Conley JR, Pampanin S (1999) Preliminary results and conclusions from the PRESSS five-story precast concrete test Building. PCI J 44(6):42–67

Roudsari MS, Pak M (2013) Ladybug: a parametric environmental plugin for grasshopper to help designers create an environmentally-conscious design. 13th IBPSA Conference. Lyon, France

Sarti F, Palermo A, Pampanin S (2016a) Fuse-type external replaceable dissipaters: experimental program and numerical modelling. J Struct Eng 142. https://doi.org/10.1061/(ASCE)ST.1943-541X.0001606.12);04016134

Sarti F, Palermo A, Pampanin S (2016b) Quasi-Static Cyclic testing of Two-Thirds scale unbonded post-tensioned rocking dissipative timber walls. J Struct Eng 142. https://doi.org/10.1061/(ASCE)ST.1943-541X.0001291

Shen X, Singhvi A, Mengual A, Spastri M, Watson V (2018) Evaluating the multi-objective optimization methodology for performance-based building design in professional practice. ASHRAE and IBPSA, pp 646–653

Smith T, Ditommaso R, Carradine D, Ponzo FC, Pampanin S (2012) Seismic performance of a post-tensioned LVL building subjected to the Canterbury earthquake sequence. NZSEE Conference. Christchurch, New Zealand

Smith T, Wong R, Newcombe MP, Carradine D, Pampanin S, Buchanan A, et al (2011) The demountability, relocation and re-use of a high-performance timber building. 9th PCEE Conference. Auckland, New Zealand

Standard New Zealand (2004) NZS 1170.5:2004 - Structural design actions: Part 5. Earthquake actions. Wellington, New Zealand

Stanton J, Stone WC, Cheok GS (1997) A hybrid reinforced precast frame for seismic regions. PCI J 42(2):20–32

Steico (2017) STEICO LVL - Elementi costruttivi in Legno. Feldkirchen, Austria

United Nations (2015) A/RES/70/1. Transforming our world: the 2030 agenda for sustainable development. United Nations (UN), New York

Vamvatsikos D (2012) Derivation of new SAC/FEMA performance evaluation solutions with second-order hazard approximation. Earthq Eng Struct Dyn 42:1171–1188. https://doi.org/10.1002/eqe.2265

Vamvatsikos D, Cornell CA Incremental dynamic analysis. Earthq Eng Struct Dyn 31:491–514., Zhu M, McKenna F, Scott MH (2018) OpenSeesPy: Python library for the OpenSees finite element framework. SoftwareX 2002. 7:6–11

Zitzler E, Laumanns M, Thiele L (2001) SPEA2: Improving the strength Pareto evolutionary algorithm. TIK-report 103

Authors and Affiliations

Giada Formichetti[1] · Giuseppe Loporcaro[2] · Stefano Pampanin[1]

✉ Giada Formichetti
giada.formichetti@uniroma1.it

[1] Department of Structural and Geotechnical Engineering, Sapienza University of Rome, Rome, Italy

[2] Department of Civil and Environmental Engineering, University of Canterbury, Christchurch, New Zealand